Solubilization of Renewable Phosphorus Sources with Organic Acids Produced by *Bacillus megaterium*

Małgorzata Wyciszkiewicz, Agnieszka Saeid* and Katarzyna Chojnacka

Department of Advanced Material Technologies, Faculty of Chemistry, Wroclaw University of Science and Technology, Gdańska 7/9, 50-344 Wrocław, Poland

Received October 10, 2016; Accepted March 09, 2017

ABSTRACT: The aim of this work was to evaluate the effects of using *B. megaterium* in solubilization of phosphates from different secondary raw materials, such as fish bones, poultry bones, ashes and phosphorite, by identification of the effect of different doses of phosphorus-bearing materials on the growth of microbial cells and the effectiveness of the solubilization process. Both FTIR as well as SEM-EDX techniques were used to compare the effect of the acids on renewable phosphorus source. Two doses of mentioned materials were used: 2 and 30 g/L. The effect of solubilization was expressed as the solubilization factor (SF, %), defined as the ratio (expressed as percentage) of soluble P_2O_5 present in the solution and total phosphorus (expressed as P_2O_5) introduced into solubilization medium in the solid form. The evaluated SF ranged between 0.672% obtained for phosphorite (30 g/L) and 85% for fish bones (2 g/L) with variations among different sources of phosphate and different doses used in the experiment.

KEYWORDS: *Bacillus megaterium*, bone, fish bone, ash, phosphorite, microbial solubilization

1 INTRODUCTION

Recent increases in global prices of phosphate rock, together with the need to remove phosphorus (P) from wastewater to control and avoid eutrophication, make phosphorus recovery economically and environmentally important [1]. Apatite and phosphorite minerals are the main nonrenewable raw materials used in the manufacturing of fertilizers [2]. The results show that 70% of global production currently comes from reserves which will be depleted within 100 years [3]. As an alternative to phosphorus rock, phosphorus can be recycled from phosphorus-rich residues such as meat and bone meal (MBM), municipal sewage sludge, phosphorus-rich ashes, and agricultural residues [4]. Today, only about one fourth of the P applied to agricultural fields is actually recycled [5]. Sustainable, innovative recycling and reuse technology methods, where the phases of the phosphate-bearing materials would be transformed into plant available phosphates, need to be developed and implemented. What is more, the obtained product should be characterized by high bioavailability and a toxic element fraction below the limit values of the fertilizer directive, thus fulfilling the quality parameters for a P-fertilizer [6].

Recovery of phosphorus from renewable resources can be carried out through an extraction procedure, such as acid leaching or electrodialysis [5], to liberate the phosphorus trapped in an unavailable form such as apatite in the case of bones, fish bones, meat bone meal (MBM) and bone meal (BM). Organically bound phosphates, similar to those present in the sewage sludge from wastewater treatment plants that perform the III° stage of the biological treatment stage (P is usually immobilized and polymerized in granules inside the cells in sewage sludge during wastewater treatment by phosphate-accumulating organisms), can be found in the MBM and BM. Due to the low boiling points of organic phosphorus compounds, it is assumed that these are released as gaseous phosphorus oxides in the furnace, for example, in the incineration of sludge where ashes enriched with phosphorus are obtained. The phosphorus oxides are condensed in the temperature range of 400–600 °C, forming primarily phosphorus-oxide, P_4O_{10}, and, in the likely presence of water, orthophosphoric acid, H_3PO_4 [4].

*Corresponding author: agnieszka.saeid@pwr.edu.pl

DOI: 10.7569/JRM.2017.634132

The utilization of the phosphorus-bearing secondary substrates as fertilizer on arable land is also possible after a digestion step performed by the use of acids. The acid digestion can be performed by synthetic acids as well as natural acids produced by microorganisms. Bacteria and fungi that can produce acids are classified as phosphate solubilizing bacteria (PSB) and phosphate solubilizing fungi (PSF) and both as a phosphate solubilizing organism (PSO). What is more, the type of synthesis by microorganism acids varies depending on the type of growth medium component used (the environment of bacterial growth) [7]. Some of the agriculture or food industry secondary phosphorus sources contain considerable amounts of phosphorus, together with organic matter and other plant nutrients such as nitrogen, sulphur and potassium presented in organic form such as bones, fish bones and slaughterhouse wastes.

Usually, one gram of fertile soil contains 10^1–10^{10} bacteria, and their live weight may exceed 2000 kg ha^1. The utilization of the ability of PSB that are ubiquitous with variation in forms and population in different soils [8] to liberate the phosphorus is a sustainable approach to the phosphorus problem. At present, the challenge is to develop an efficient method which has low impact on the environment and is economical as well.

The aim of this work was to evaluate the effects of application of soil bacteria *B. megaterium* in the solubilization process of phosphates from different secondary phosphorus-bearing raw materials, such as fish bones, poultry bones, ashes and phosphorite, by the identification of the effect of different doses of materials used in the experiment on the growth of microbial cell, the changes of pH value, the amount of solubilized phosphorus (expressed as P_2O_5) as well as the effectiveness of the solubilization process. Both FTIR and SEM-EDX techniques were used to compare the effect of the acids on the secondary phosphorus source.

2 MATERIAL AND METHODS

2.1 Bacteria and Culture Medium

Phosphate sources were treated with *Bacillus megaterium* (PCM 1855) as a phosphate-solubilizing microorganism. Bacteria were obtained from the Polish Collection of Microorganisms located at the Institute of Immunology and Experimental Therapy in Wroclaw (WDCM106). For cultivation of bacteria, growth medium was described previously [9].

2.2 Phosphate Source

In solubilization experiments, the phosphate sources used were poultry cooked bones, fish bones, ash from wastewater sludge (originating from Łyna plant in Olsztyn, Poland), as well as Morocco phosphate rock (phosphorite). All phosphate substrates were ground with a blender and sieved to pass through 1 mm particle size fractions for chemical and solubilization studies.

2.3 Extraction of P_2O_5

In order to investigate the efficiency and consequently bioavailability of phosphorus (expressed as P_2O_5) from phosphate sources used in experiments, ammonium citrate and water extracts were determined as described previously [10].

2.4 Experimental and Analytical Methods

The solubilization experiment was conducted in Erlenmeyer flasks (capacity 500 mL) with 250 mL medium and 2 g and 30 g per 1L of phosphate source at 34 °C under sterile conditions. The medium solution with the phosphorus sources was inoculated with bacteria from agar slant by inoculating loops and incubated as batch cultures. During 8 days of cultivation/solubilization, culture medium was shaken at 120 rpm and incubated at 34 °C (Gerhardt Thermoshake incubator shaker). Samples of microorganism suspension from all culture groups (four groups: poultry cooked bone, fish bones, ash from wastewater sludge and Morocco phosphate rock) were collected at the same time. The reaction mixture was filtered through filter paper and permeates were used for the estimation of pH and P_2O_5 concentrations, which were measured by colorimetric vanadophosphomolybdate method. At the end of the experiment, the solids separated through filtration were analyzed by FTIR and SEM-EDX. The pH measurements were conducted with a Mettler Toledo SevenMulti pH meter equipped with an electrode InLab 413 with compensation of temperature.

2.5 Cell Growth

The biomass concentration of *B. megaterium* was measured spectrophotometrically as described previously [11].

2.6 Fourier Transform Infrared (FTIR) Spectroscopy

The FTIR spectroscopy technique was used to identify functional groups present on the surface of phosphorus-bearing materials. Before analyzation, a few milligrams of material were ground and mixed with potassium bromide disks in an amount provided

by the material at concentration of 2% by mass. The FTIR spectra of prepared samples were collected using a PerkinElmer System 2000 (Waltham, MA, USA) equipped with a deuterated triglycine sulfate (DTGS) and mercury cadmium telluride (MCT) detector. The assay was conducted within the wavenumber range of 400–4000 cm^{-1} (mid-infrared region) using a potassium bromide window at room temperature (°C). The FTIR spectra were elaborated with a System 2000 compatible software (PerkinElmer, Waltham, MA, USA), which was used to perform the background calculation in order to set the necessary entries for result assessment. Obtained background, corresponding to pure potassium bromide (KBr), was automatically subtracted from each sample spectrum. All spectra were plotted using the same scale on the transmittance axis.

The area under the FTIR spectrum as a measure of the amount of phosphates in the phosphorus-bearing materials was calculated from Equation 1 where: A is absorbance and is wavenumber, cm^{-1}, i = 2, 3, 4… are the next measurements of wavenumber in the range of absorbance from 900 to 1200 cm^{-1}.

$$\text{area under the FTIR spectrum } \left(A_{900}-A_{1200}\right) = \int_{900}^{1200} f\left(\tilde{v}\right)d\tilde{v} = \Sigma_i\left[\left(v_i-v_{i-1}\right)\cdot\left(\frac{\left(1-A\right)_i+\left(1-A\right)_{i-1}}{2}\right)\right] \quad (1)$$

2.7 Scanning Electron Microscopy with Energy-Dispersive X-Ray (SEM-EDX) Analytical System

Physical and morphological characterizations were performed on phosphrous-bearing materials before and after solubilization by scanning electron microscopy with energy-dispersive X-ray analysis (SEM-EDX). A total of twelve samples of phosphorus-bearing materials were fixed in 2.5% of glutaraldehyde (Sigma-Aldrich, http://www.sigmaaldrich.com/) and next were dehydrated by ethanol (from 30% till 100% concentration). Treated mass was sampled and prepared in two planes, enabling observation of the cross section and its surface. All samples were mounted onto a proper stub and afterwards gold sputtered using HHV Scancoat Six equipment (Crawley, Oxfordshire, UK). Observation and images of microalgae surface composition were taken with a Zeiss LEO 435 VP SEM scanning electron microscope (Oberkochen, Germany), operating at 20 kV. The concentration of particular surface constituent was recorded using a RÖNTEC GmbH energy-dispersive X-ray system (Berlin, Germany) as additional microscope equipment. As a result, the X-ray spectra of elemental composition, specific for natural acids and solubilized by bacteria surface were obtained.

2.8 Calculations

The arithmetic mean values, standard deviations (SD) and *t* tests, as well as the model parameters of equations describing the experimental data, were determined using nonlinear estimation and multiple regression modules of Statistica software version 9.0. Correlation was considered statistically significant at $\alpha < 0.05$.

Chi-square test (χ^2 test) was also used, which was calculated from Equation 2, which more accurately described the fit of the model to experimental data compared to the determination coefficient R^2.

$$\chi^2 = \frac{\left(\text{experimental value} - \text{model value}\right)^2}{\text{model value}} \quad (2)$$

3 RESULTS

3.1 Growth of *Bacillus megaterium*

The specific growth rate of *B. megaterium* in four different medium compositions and solubilization factor evaluated for different phosphorus materials and different doses are presented in Table 1. It was found that in the case of organic phosphorus-bearing materials, such as poultry bones and fish bones, growth rate was higher when the doses of materials used in the

Table 1 The specific growth rate of *B. megaterium* in four different medium compositions and solubilization factor evaluated for different phosphorus materials and different doses.

Raw material		*SF*, %	ΔpH	μ, 1/day	R^2
Poultry bones	**2 g/L**	77.8	–2.071	3.25	0.896
	30 g/L*	21.9	–1.52	2.15	0.679
Fish bones	**2 g/L**	85.0	–1.703	2.76	0.973
	30 g/L*	24.7	–2.17	2.09	0.767
Ash	**2 g/L**	42.8	–2.40	1.72	0.984
	30 g/L*	16.2	–1.7	1.83	0.702
Phosphorite	**2 g/L**	29.1	–2.43	1.86	0.872
	30 g/L*	0.672	–0.143	1.905	0.977

*[7]

experiment were lower (2 g/L) when compared with the higher dose of 30 g/L.

3.2 Concentration of P_2O_5

The changes of phosphorus (expressed as the P_2O_5) concentration during solubilization process performed by *B. megaterium* with the utilization of four different phosphorus raw materials are presented in Figure 1a. The influence of different doses on the solubilization of various phosphorus-bearing materials was presented by a model that describes the kinetics of phosphorus release (expressed as the P_2O_5) (Equation 3):

$$C_{P_2O_5} = f(t) = \frac{C^{max}_{P_2O_5}}{1 + b \cdot \exp^{-k \cdot t}} \quad (3)$$

where the $C^{max}_{P_2O_5}$, *mg/L* is the maximum concentration of P_2O_5, *b* is the constant that expresses time when is C_{P_2O5} equal to ½ of $C^{max}_{P_2O_5}$ and *k* is the *1/day* constant is the variable slope, which is called the Hill slope. When *k* is greater the curve changes more sharply, which means that the solubilization process proceeds faster. Table 2 collects the evaluated values of all parameters of the proposed model, as well as the *p*-value and errors that express the fit of the model to the experimental data. The highest maximum P_2O_5 concentration was found for poultry bones and fish bones, 310 mg/L and 230 mg/L, respectively (Table 2, Figure 1a). The content of phosphorus (expressed as P_2O_5) in used materials varies, the total P_2O_5, mg/kg was 12.8, 19.6, 13.5 and 34.2 for poultry bones, fish bones, ash and phosphorite, respectively. While the available P_2O_5 was mg/kg 0.0185, 0.0389, 0.14 and 0.0205 for poultry bones, fish bones, ash and phosphorite, respectively.

3.3 pH

The relationship between pH value and phosphorus (expressed as P_2O_5) concentration in the solubilization process performed by *B. megaterium* with the utilization of four different phosphorus raw materials is shown in Figure 1b. The solubilization of phosphorus-bearing sources by *B. megaterium* strain was accompanied by a significant drop in pH for 2 g/L of phosphorus sources to 4.59, 4.50, 4.85 and 4.60 from an initial pH of 6.66, 6.20, 7.27 and 7.002 after 8 days for poultry bones, fish bones, ash and phosphate rock, respectively. In the case of a dose of 30 g/L of phosphorus sources, a decrease was also observed with the exception of phosphorite, where a slight increase of pH was observed [7].

The P_2O_5 concentration is correlated with the pH of the liquid phase through the following equation (Figure 1b):

$$pH = f\left(C_{P_2O_5}\right) = \frac{A + pH_{min} \cdot C_{P_2O_5}}{C_{P_2O_5}} \quad (4)$$

where *A*, mg/L is a constant describing the decay of the curve. Evaluated value of pH_{min} can be interpreted as the minimal value of pH. A strong correlation was found between pH and soluble P_2O_5 concentration. The parameters of the proposed model as well as the *p*-value and errors that express the fit of the model to the experimental data are presented in Table 3 for the concentration 2 g/L; additionally, the data from previous experiments performed for the concentration 30 g/L published elsewhere [7] are presented to compare the effect of different doses.

3.4 FTIR

Figure 2 shows the FTIR spectra of samples of different phosphorus-bearing materials before and after solubilization undertaken at different conditions (different doses of material). It can be found that the characteristic bands for PO_4^{3-} group consist of three main regions marked in Figure 2 as *A*, *B* and *C*. The first region (region *A* in Figure 2a-bones) is represented by the peaks 1095, 1037 cm^{-1} corresponding to stretching mode and 958 cm^{-1} associated with stretching mode. The second region (region *B* in Figure 2a) of phosphate ions is represented by the band with well-defined peaks at 667, 603 and 563 cm^{-1} corresponding to bending mode. The third region (region *C* in Figure 2a) is observed at 468 cm^{-1}, exhibiting weak bands corresponding to bending mode [12–14]. Values representing the phosphorus valuated from Equation 1 are presented in Table 4.

Hydroxyl stretching mode is observed on all sample spectra 3000–3700 cm^{-1} represented by very low intensity peaks in the case of phosphate rock and ash and high intensity in the case of bones and fish bones. Observed broad band can be assigned to different structural OH groups in HAp crystals (–OH groups with more or less hydrogen bond association with phosphate groups, and others with less or no interactions with the environment) [13, 15, 16].

Concerning carbonate ions, there are usually three vibrational bands which can be observed in the infrared spectra of bone and hydroxyapatite, but bands exhibit very low intensity and are rarely observed. In analyzed samples, carbonate ions were detected in two different sites: a) low intensity peak at 880 cm^{-1} attributed to the CO_3^{2-} group and characteristic of a

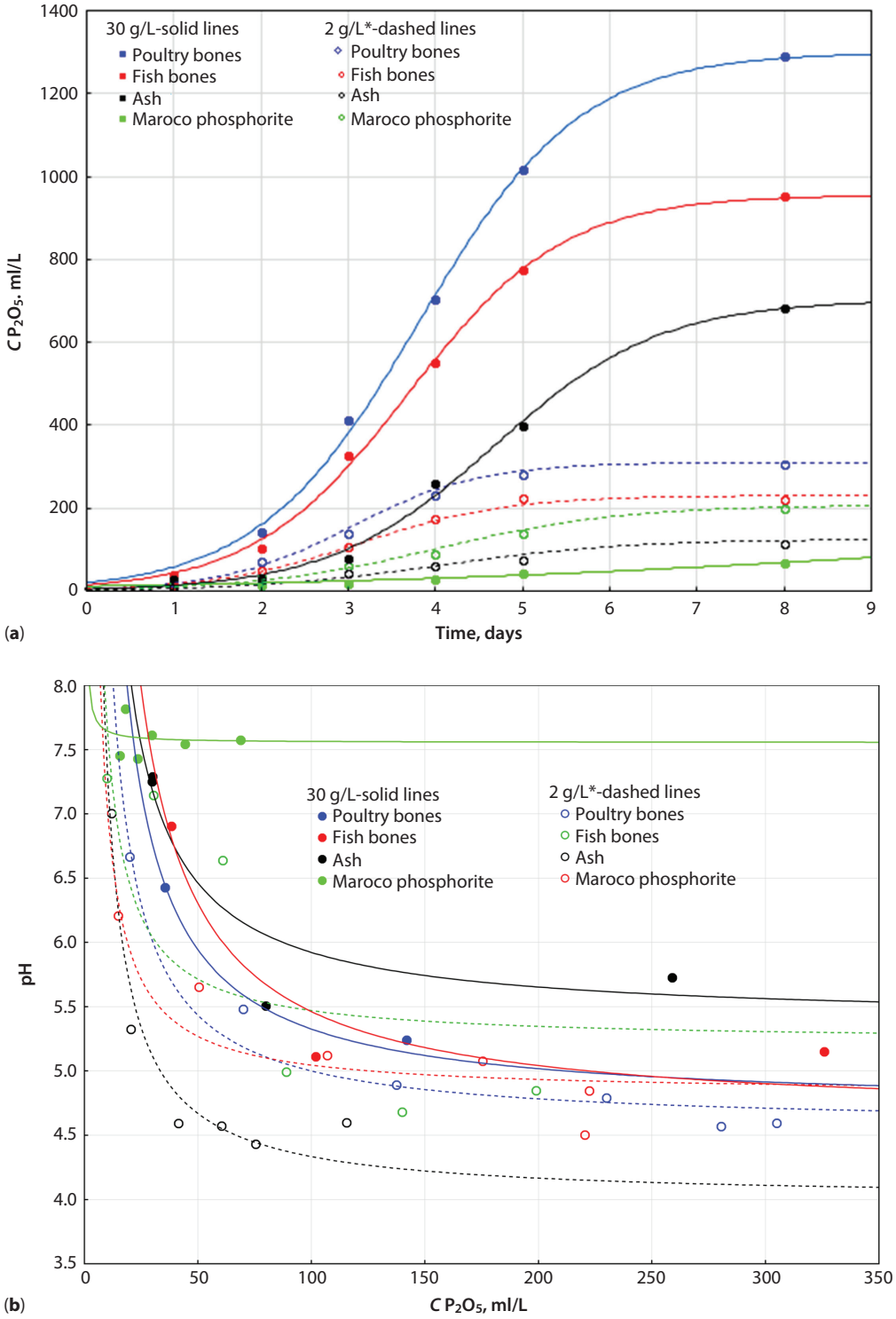

Figure 1 (**a**) Changes of phosphorus (expressed as the P_2O_5) concentration during solubilization process performed by *B. megaterium* with the utilization of four different phosphorus raw materials. (**b**) Relationship between pH and phosphorus (expressed as P_2O_5) concentration in the solubilization process performed by *B. megaterium* with the utilization of four different phosphorus raw materials.

Table 2 Parameters of model describing the kinetics of changes of concentration P_2O_5 during the solubilization process.

Phosphorus raw material	2 g/L						30 g/L*				
	Parameters		SD	*p* value	R^2	χ^2	Parameters	SD	*p*-value	R^2	χ^2
Poultry bones	$C^{max}_{P_2O_5}$, *mg/L*	310	26	0.000272	0.987	30.5	1299	28	0.000022	0.999	13.9
	b, day	60.3	5.5	0.0725			0.471	0.028	0.000466		
	k, 1/day	1.35	0.146	0.00669			3.81	0.07	0.000014		
Fish bones	$C^{max}_{P_2O_5}$, *mg/L*	230	12	0.000043	0.993	14.9	955	21	0.000024	0.999	6.96
	b, day	40.5	12.8	0.107			0.488	0.031	0.000558		
	k, 1/day	1.18	0.18	0.00338			3.69	0.07	0.000017		
Ash	$C^{max}_{P_2O_5}$, *mg/L*	125	10	0.000220	0.995	14.9	703	31	0.000186	0.997	28.3
	b, day	44.1	3.9	0.0217			0.456	0.059	0.00452		
	k, 1/day	0.931	0.096	0.00275			4.68	0.15	0.000073		
Phosphorite	$C^{max}_{P_2O_5}$, *mg/L*	207	27	0.000873	0.993	10.8	188	511	0.737	0.959	7.79
	b, day	46,3	3.7	0.0113			0.117	0.099	0.324		
	k, 1/day	0.951	0.088	0.00330			10.0	17.4	0.607		

*[7]

Table 3 Parameters of model describing the changes of pH and P_2O_5 concentration during the solubilization process.

Phosphate sources	2 g/L						30 g/L*				
	Model parameters		SD	*p* value	R^2	χ^2	Model parameters	SD	*p*-value	R^2	χ^2
Poultry bones	*A*, mg/L	43.4	4.4	0.000596	0.979	0.0253	61.7	4.8	0.000204	0.988	0.0107
	pH_{min}	4.57	0.10	0.000001			4.71	0.06	0.000000		
Fish bone	*A*, mg/L	22.3	5.6	0.0161	0.89	0.0723	84.0	11.1	0.001617	0.966	0.046
	pH_{min}	4.82	0.16	0.000007			4.62	0.13	0.000003		
Ash	*A*, mg/L	33.5	4.1	0.00128	0.73	0.599	53.9	8.9	0.003872	0.949	0.0611
	pH_{min}	4.00	0.17	0.000021			5.38	0.18	0.000007		
Phosphorite	*A*, mg/L	24.5	11.5	0.0994	0.97	0.0567	0.407	3.69	0.917344	0.055	0.0127
	pH_{min}	5.22	0.50	0.000483			7.55	0.16	0.000001		

*[7]

carbonated apatite (with the substitution of PO_4^{3-} by CO_3^{2-} ions in the apatite structure [15] and b) peaks from 1639 to 1384 cm^{-1} [12, 16–18].

Bands appearing at wavenumber values of 2855 and 2925 cm^{-1} were assigned to the absorption of organic material [12]. Additionally, the bands of C1⁄4O and C1⁄4C (protein and collagen) were assigned to the peaks at 1500–1600 cm^{-1} corresponding to the organic phase of bone material. These peaks disappear in the case of ash and phosphorite, indicating their removal from the bone material during pyrolysis in the case of ash and phosphogenesis in the case of phosphate rock [14, 19].

3.5 SEM-EDX

The scanning electron micrographs are shown in Figure 3. EDX analysis was performed and the results are shown in Figure 5 and Table 5.

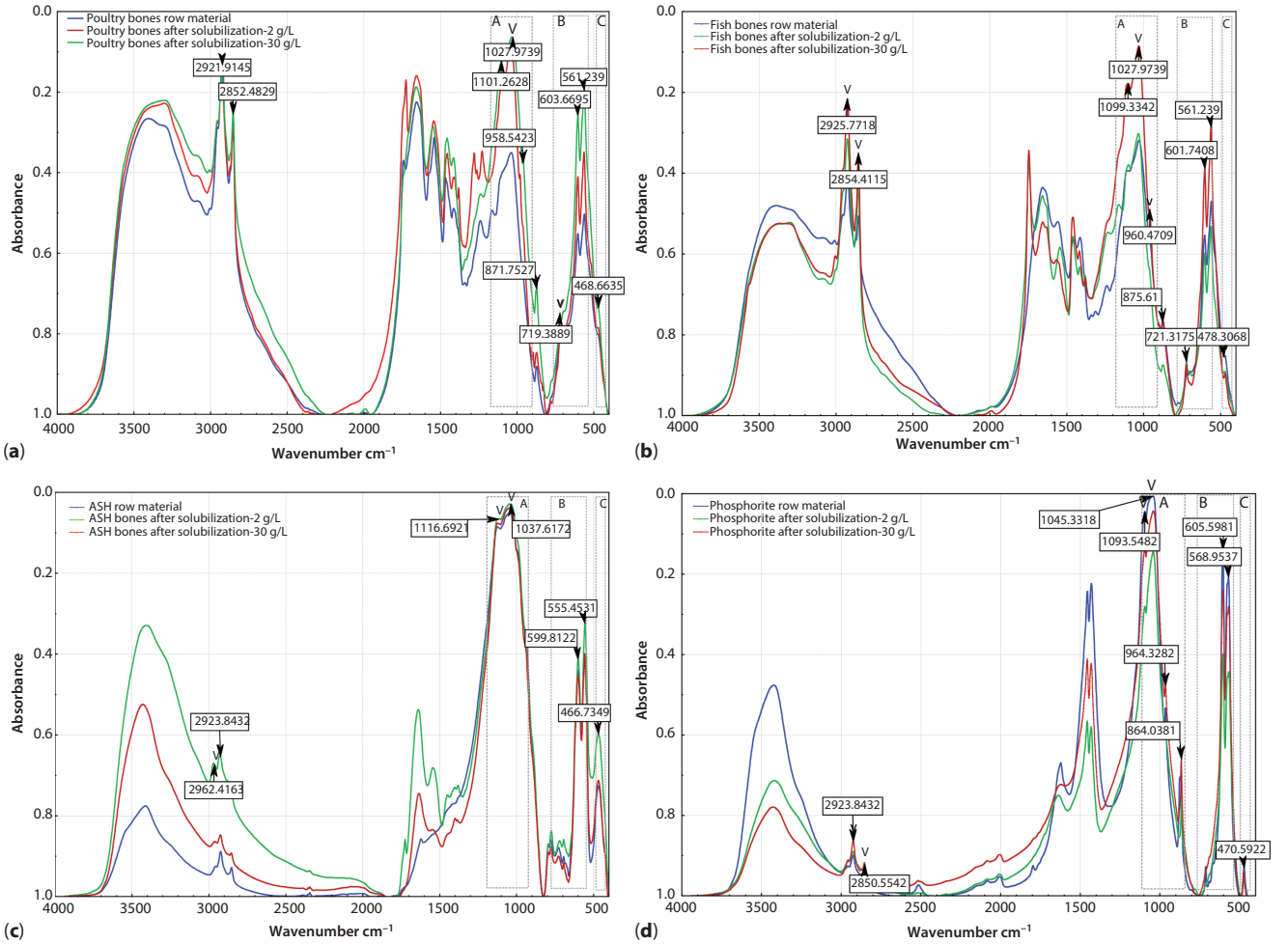

Figure 2 Normalized FTIR absorption spectrum of selected functional groups exposed on the surface of phosphorus-bearing materials: (**a**) poultry bones, (**b**) fish bones, (**c**) ash and (**d**) phosphorite.

Table 4 The area under the FTIR spectrum as a measure of the amount of phosphates in the phosphorus-bearing materials (calculated from Equation 1).

Raw material		$\int_{900}^{1200} f(\tilde{v})d\tilde{v}$
Poultry bones	raw	142.26
	2 g/L	189.69
	30 g/L	217.15
Fish bones	raw	151.05
	2 g/L	146.68
	30 g/L	196.34
Ash	raw	242.04
	2 g/L	244.31
	30 g/L	237.31
Phosphorite	raw	187.00
	2 g/L	158.56
	30 g/L	189.25

4 DISCUSSION

The solubilization process was performed for two different doses of phosphorus-bearing materials, 2 and 30 g/L. Selection of concentrations was made based on the previous research that confirmed the strong relationship between solubilization factors and applied in the experiment doses of materials used as a source of phosphorus. With increased doses the decrease of solubilization factor was observed [10], which is why the two extreme doses were chosen. The effect of solubilization was expressed as the solubilization factor (SF, %), defined as the ratio (expressed as percentage) of soluble P_2O_5 present in the solution and phosphorus (expressed as P_2O_5) introduced into solubilization medium in the solid form.

The efficient growth of bacteria is crucial in solubilization of phosphorus-bearing materials. Bacteria are responsible for production of organic acids that are the main factor that affects the release of

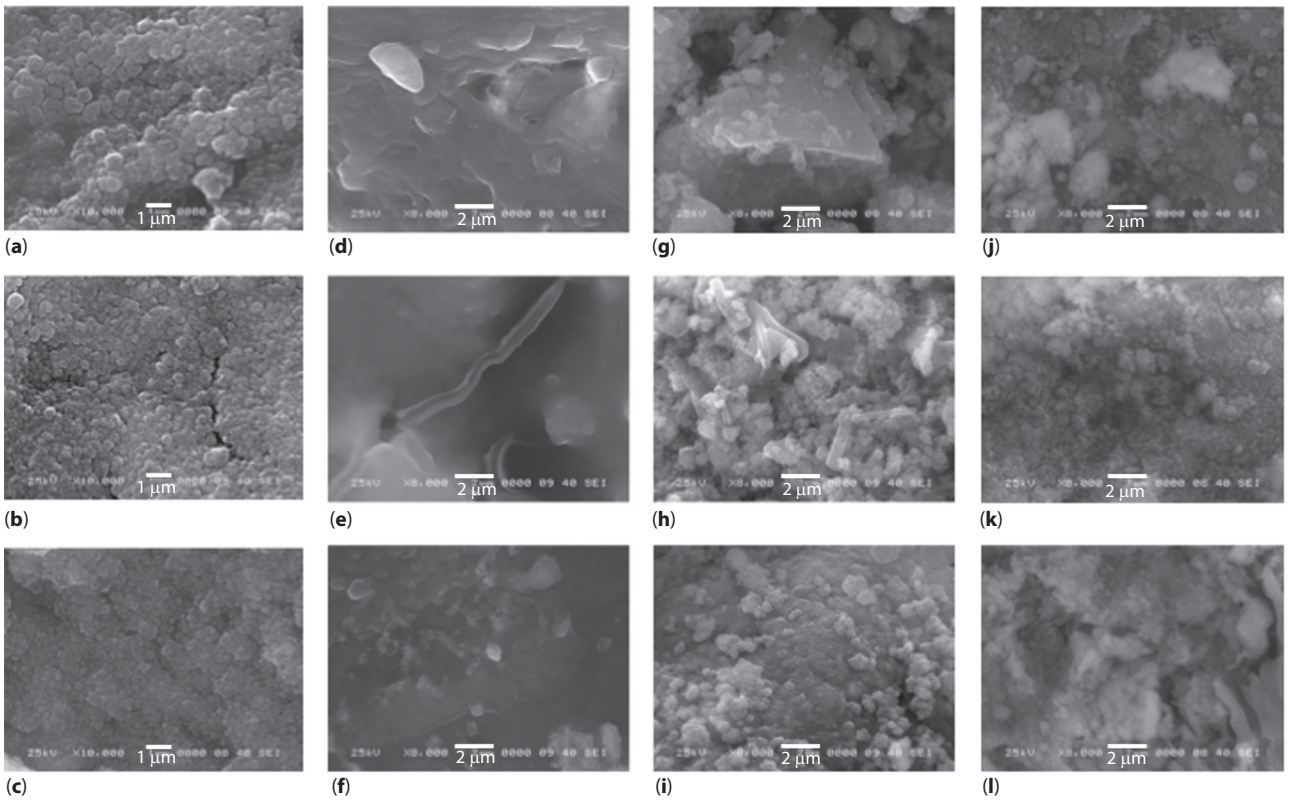

Figure 3 The surfaces of poultry bones untreated (**a**) and poultry bones exposed to solubilization process (2 g/L [**b**]; 30 g/L [**c**]). The surfaces of fish bones untreated (**d**) and fish bones exposed to solubilization process (2 g/L [**e**]; 30 g/L [**f**]). The surfaces of ash untreated (**g**) and ash exposed to solubilization process (2 g/L [**g**]; 30 g/L [**i**]). The surfaces of phosphorite untreated (**j**) and phosphorite exposed to solubilization process (2 g/L [**k**]; 30 g/L [**l**]. Scale bar 1 µm for a, b, c, and 2 µm for d, e, f, g, h, i, j, k, l.

phosphorus from the apatite structure. The monitoring of its growth and providing appropriate conditions for growth ensure efficient solubilization. Too high of a dose of nutrients delivered in the form of poultry bones as well as fish bones decreases the growth of bacteria, which confirmed that this form of nutrients is more available for microbial cells when compared with inorganic substrates (such as ash and phosphorite). Substrate inhibition of microbial growth is well documented, but experiments evaluating the effect of dose of substrate on the growth should be performed to evaluate the specific growth rate by the application of Monod (without substrate growth inhibition) or Haldane (with substrate growth inhibition) models [20]. Different phenomena were recognized in the case of inorganic materials, such as ash and phosphorite, when the dose did not affect the growth of bacteria (Table 1). This finding could be explained as a reason for the form of nutrients delivered in that inorganic form which is probably not available for bacterial cells; therefore, even if the dose of substrate increases, no effect would be observed.

Although the effect on the growth of bacteria was not noticeable only in the case of phosphorite, the inhibition of solubilization caused by a higher dose of material was observed (the was lower for the dose of phosphorite 30 g/L when compared with the obtained for 2 g/L). In all considered cases the increase of dose of material used as a source of phosphorus resulted in a decrease of solubilization factor for 2 g/L 77.8, 85.0, 42.8 and 29.1 for poultry bones, fish bones, ash and phosphate rock, respectively, while for 30 g/L the following solubilization factor was evaluated: 21.9%, 24.7%, 16.19% and 0.672%.

According to our previous studies, during the solubilization process performed by *B. megaterium*, different organic acids were produced and their composition was strongly related to the material used as a source of phosphorus [10]. Acids produced by bacteria caused an increase of concentration of hydrogen ions and higher release of P_2O_5. It can be found that in all considered cases, with the exception of fish bones, the increase of doses of phosphorus-bearing material resulted in the higher value of evaluated parameter pH_{min}. These phenomena can be explained by the more

abundant presence of substances originating from materials used as a source of phosphorus that neutralized the protons produced by bacterial cells in the solubilization process.

Obtained parameters, such as , pH_{min}, μ, SF, and ΔpH, used for describing the data were statistically tested to find whether they are correlated. A statistically significant correlation between *SF* and pH_{min} (r = 0.809, p = 0.0148) was found for data obtained for 2 and 30 g/L (n = 8). Moreover, a statistically significant correlation was found between *SF* and pH_{min} (r = 0.927, p = 0.073), between and μ (r = 0.908, p = 0.092) and between pH_{min} and μ (r = −0.931, p = 0.069) when only the dose of 2 g/L was taken into consideration (n = 4). Additionally, a statistically significant correlation was found between *SF* and pH_{min} (r = 0.953, p = 0.047), between and *SF* (r = 0.606, p = 0.094) and between pH_{min} and μ (r = 0.939, p = 0.061), when the dose of 30 g/L was taken into consideration (n = 4).

Raw phosphorus-bearing materials and materials after microbial solubilization performed at the different doses did not show large differences in FTIR spectra (Figure 2), which suggested that the chemical structures were not significantly affected by the performed process; nevertheless, the differences in the intensity of peaks, particularly in the region that determines the presence of phosphate groups, were noticeable. According to Pienkowski *et al.* [21], the band intensity can be evaluated as a relative amount of detected groups and the changes in the FTIR spectra could be explained as changes of the amount of present groups that were detected on the surface as a result of the action of organic acids produced by *Bacillus megaterium* in the biosolubilization process. The broad bands between 900 and 1200 cm^{-1} are attributed to the symmetric and asymmetric stretching vibrations (O-P-O) of the PO_4^{3-} group, as mentioned by Bonadio *at al.* [16]. According to Álvarez-Lloret *et al.* [22], the surface area under the graph in that range was used as a measure of the amount of phosphates in analyzed materials (Equation 1). In the case of poultry bones, the solubilization resulted in an increased amount of phosphates present on the surface as an effect of dissolution of the outer part of the surface by the action of organic acids. In the case of fish bones, a small decrease of phosphates after the solubilization (at fish bone concentration 2 g/L) was observed and an increase in the amount of 30% was observed when compared to the raw samples. While in the case of organic materials (poultry bones and fish bones) the effect of solubilization and influence of different doses were noticeable, the FTIR spectra of ash and phosphate rock in the range of A_{900}-A_{1200} did not show significant changes.

The scanning electron micrographs are shown in Figure 3. After the solubilization was performed at the dose of 30 g/L, surface changes are barely visible or not visible, which is consistent with previous findings concerning the influence of the doses used on the estimated solubilization factor. A lower dose caused higher SF, so a higher amount of phosphorus from the hydroxyapatite structure was released and a stronger effect on the surface could be expected. Scanning electron microscopy (SEM) analysis of the solid material after biosolubilization performed at 2 g/L showed more surface erosion of the biologically leached material than observed in the untreated and treated (30 g/L) material. Figure 4 presents the optical microscopy images of poultry and fish bones before

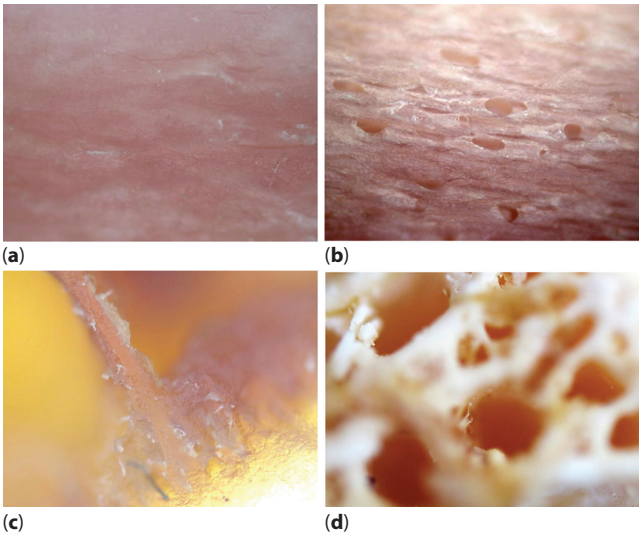

Figure 4 The optical microscopy (10x) image of poultry (**a**) before the solubilization and (**b**) after 7 days of solubilization; bones and fish bones (**c**) before the solubilization and (**d**) after 7 days of solubilization.

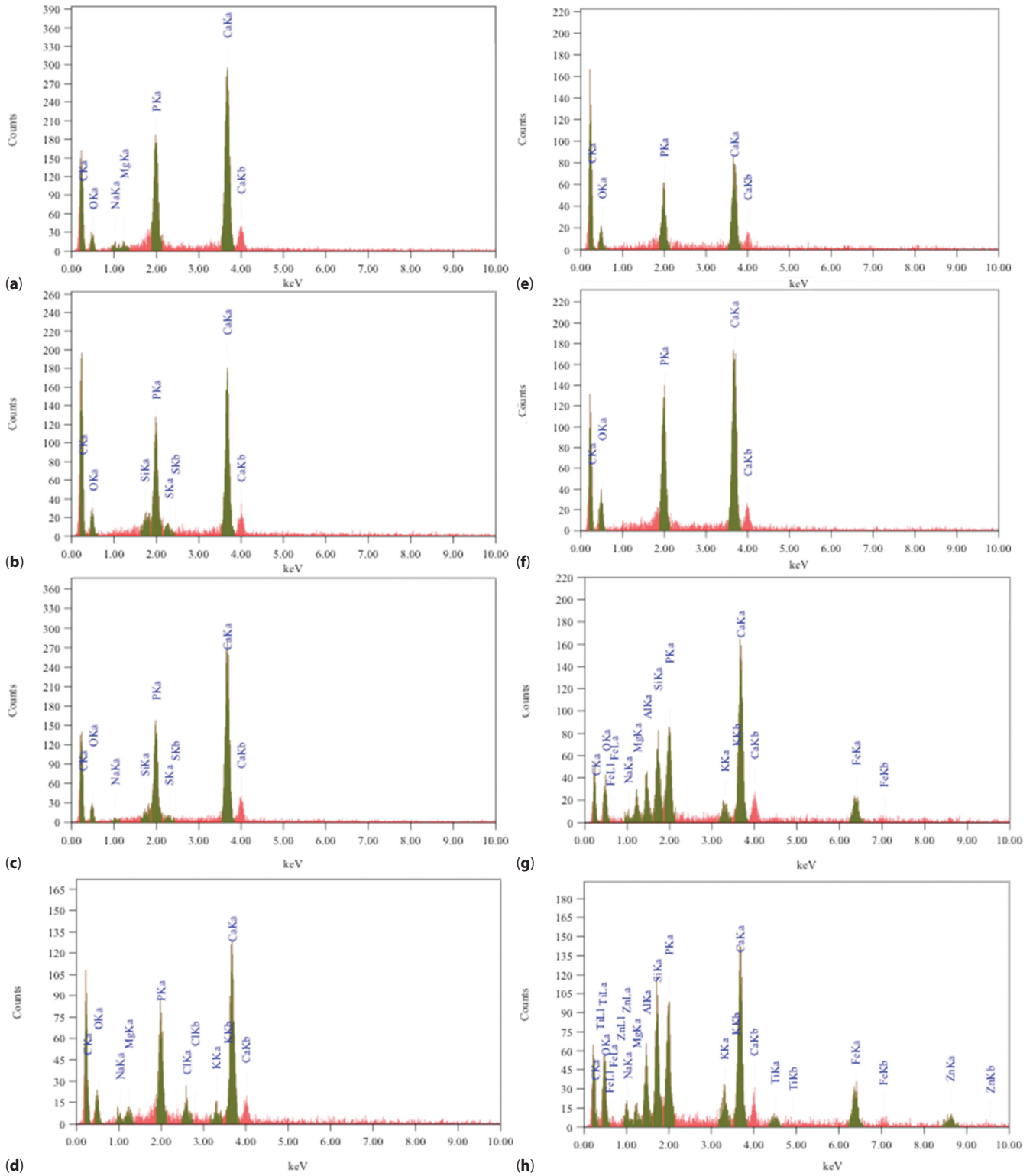

Figure 5 EDX results for poultry bones untreated (**a**) and poultry bones exposed to solubilization process (2 g/L [**b**]; 30 g/L [**c**]). EDX results for fish bones untreated (**d**) and fish bones exposed to solubilization process (2 g/L [**E**]; 30 g/L [**f**]). EDX results for ash untreated (**g**) and ash exposed to solubilization process (2 g/L [**g**]; 30 g/L [**i**]). EDX results for phosphorite untreated (**j**) and phosphorite exposed to solubilization process (2 g/L [**k**]; 30 g/L [*l*]). (*Continued*)

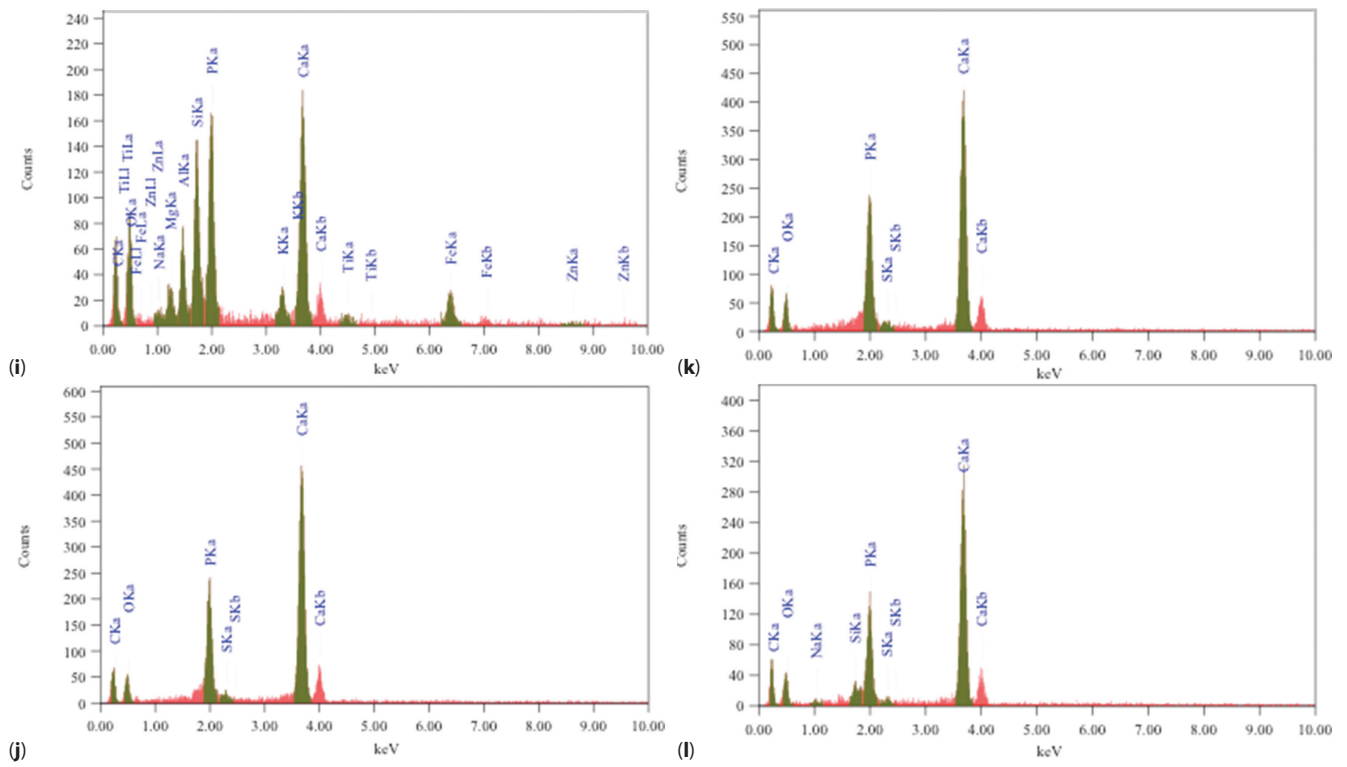

Figure 5 EDX results for poultry bones untreated (**a**) and poultry bones exposed to solubilization process (2 g/L [**b**]; 30 g/L [**c**]). EDX results for fish bones untreated (**d**) and fish bones exposed to solubilization process (2 g/L [**e**]; 30 g/L [**f**]). EDX results for ash untreated (**g**) and ash exposed to solubilization process (2 g/L [**g**]; 30 g/L [**i**]). EDX results for phosphorite untreated (**j**) and phosphorite exposed to solubilization process (2 g/L [**k**]; 30 g/L [*l*]).

and after 7 days of solubilization (2 g/L), where significant digestion of structure is visible.

For fish bones, the most significant effect was observed on the surface after solubilization at dose 2 g/L (Figure 3d–f). It can be seen that the nodules recognized as a phosphorite [23] in the case of untreated material, disappear and appear more amorphous after the solubilization at dose 2 g/L where the highest solubilization factor was found to be 85%. These findings were not observed in the case of the surface of fish bones after the solubilization process performed at dose 30 g/L, which is confirmed by the comparable low solubilization factor (24.7%). Also, in the case of poultry bones for the samples obtained from the solubilization process performed at the dose 2 g/L, some changes can be found, such as the appearance of cracks, that demonstrate the effect of the action of acids on the structure of apatite. The hydroxyapatite nodules appear to be smaller (Figure 3b) when compared with the untreated sample (Figure 3a) (the same scale bar 1 μm). The phosphorite seems to be most resistant to the action of acids on the structure of apatite that is visible on the surface, which is confirmed by the smallest solubilization factor when compared to all considered materials. The phosphorite is the oldest, and at the same time, the most stable material, when compared with fish bones generated/built up in a few weeks or poultry bones in a few months. In the case of ash, bigger nodules can be found on the SEM graph (Figure 3g–i). The reason for such phenomena is that the thermal decomposition during combustion of sludge gives large particle size apatite. The formation of the big particles in the thermal process can be regarded as the tendency of hydroxyapatite grains to agglomerate and grow up at high temperatures [24].

The confirmation of the solubilization of phosphates present on the surface in the form of apatite can be found in the results obtained from EDX analysis. The concentrations of elements detected are expressed as mass percentages (Table 5). In the case of phosphorite, where the solubilization factor was the smallest, there were very few changes found in the concentration of phosphorus. The highest changes were found for the materials that undergo solubilization at the dose of 2 g/L, which is consistent with previous findings presented in this article. The concentration of phosphorus on the surface of poultry bones in the case of samples obtained after solubilization was lower when compare with the raw poultry bones. What is more, the concentration of phosphorus on the surface for

DOI: 10.7569/JRM.2017.634132

Table 5 Mean concentrations of elements detected and expressed as weight percentages ± SD.

Raw material C		EDX, %													
		O	Ca	P	Mg	Na	K	S	Si	Fe	Al	Zn	Cl	Ti	
Poultry bones	raw	38.20 ± 0.2	16.13 ± 1.00	32.56 ± 0.28	11.14 ± 0.15	0.92 ± 0.28	0.94 ± 0.31	–	–	–	–	–	–	–	–
	2 g/L	46.03 ± 0.22	18.58 ± 1.36	25.56 ± 0.41	8.79 ± 0.22	–	–	–	0.64 ± 0.24	0.36 ± 0.30	–	–	–	–	–
	30 g/L	38.08 ± 0.2	17.50 ± 1.01	32.97 ± 0.29	9.98 ± 0.16	–	0.51 ± 0.32	–	0.51 ± 0.17	0.45 ± 0.22	–	–	–	–	–
Fish bones	raw	4.035 ± 0.25	18.77 ± 1.24	26.45 ± 0.39	9.12 ± 0.21	0.80 ± .37	0.89 ± 0.41	1.55 ± 0.32	–	–	–	–	–	2.06 ± 0.25	–
	2 g/L	52.92 ± 0.24	20.42 ± 1.87	19.04 ± 0.6	7.63 ± 0.32	–	–	–	–	–	–	–	–	–	–
	30 g/L	37.70 ± 0.22	23.51 ± 0.97	27.53	11.26 ± 0.17	–	–	–	–	–	–	–	–	–	–
Ash	raw	25.59 ± 0.17	17.25 ± 0.42	23.27 ± 0.16	7.76 ± 0.11	3.14 ± 0.17	0.77 ± 0.20	1.53 ± 0.14	–	6.16 ± 0.14	9.50 ± 0.38	5.02 ± 0.15	–	–	–
	2 g/L	23.00 ± 0.17	20.18 ± 0.37	16.04 ± 0.14	7.55 ± 0.10	1.60 ± 0.17	0.90 ± 0.22	2.12 ± 0.12	–	8.66 ± 0.13	9.32 ± 0.32	5.12 ± 0.14	4.75 ± 0.84	–	2.12 ± 0.12
	30 g/L	21.49 ± 0.17	24.99 ± 0.32	16.59 ± 0.13	10.76 ± 0.09	1.90 ± 0.14	0.26 ± 0.18	1.94 ± 0.11	–	8.63 ± 0.11	6.68 ± 0.30	5.06 ± 0.11	1.04 ± 0.78	–	0.67 ± 0.18
Phosphorite	raw	20.37 ± 0.11	23.99 ± 0.41	43.09 ± 0.12	11.85 ± 0.07	–	–	–	0.71 ± 0.07	–	–	–	–	–	–
	2 g/L	20.84 ± 0.13	28.13 ± 0.43	38.62 ± 0.14	11.99 ± 0.08	–	–	–	0.42 ± 0.09	–	–	–	–	–	–
	30 g/L	21.26 ± 0.16	25.78 ± 0.54	40.04 ± 0.17	10.31 ± 0.10	–	0.76 ± 0.21	–	0.44 ± 0.10	1.41 ± 0.13	–	–	–	–	–

samples after solubilization performed at the dose of 2 g/L was lower than for samples at the dose of 30 g/L, which remains consistent with previous findings that the dose of raw material has a crucial influence on the solubilization factor. Lower concentration of phosphorus on the surface in this case can be understood as a result of more efficient solubilization, because a higher amount of phosphorus was released from the hydroxyapatite structure. Similar findings were found for fish bones and ash, except in the case of phosphorite where it was not observed; the reason for this is the stability of the structure as a result of longer formation time when compared with other materials used in this experiment, which was discussed in the previous paragraph. Of interest is the appearance in the EDX analysis of other elements after solubilization which were not detected before, such as S, Si, Zn and Ti. Probably the solubilization of the external layers exposed the lower, inner parts that were composed of the mentioned elements, which affected their detection in the EDX analysis. In the case of carbon (C) for samples of poultry bones as well as fish bones, concentration of C after solubilization was higher, while for ash and phosphorite the concentration of C was almost the same. Probably the reason for that phenomenon is that phosphorite and ash are deprived of organic carbon.

According to the chemical formula of the standard hydroxyapatite ($Ca_{10}(PO_4)_6(OH)_2$), the theoretical calcium-to-phosphorous molar ratio is approximately 1.67 [25]. As shown, the Ca/P ratio for the phosphorus-bearing materials was higher than theoretical calcium-to-phosphorous molar ratio; nevertheless, these values lie within the acceptable range for the hydroxyapatite. Calcium-to-phosphorus ratio varied in the tested materials from 1.5 for ash after the solubilization (30 g/L) to 3.8 for phosphorite after solubilization (30 g/L). According to Jabłoński *et al.* [26], average Ca/P evaluated for bones derived from mice was 3.42. These findings are similar to those presented in this article. Additionally, the elemental analysis indicated the presence of Na, K, Mg and S, Al, Si, Zn, Ti and Fe (see Table 5). Bone does have 65–70% hydroxyapatite and 30–35% organic compounds (on a dry weight basis). Collagen is the main organic compound present in natural bone (95%), besides which there are other organic compounds existing in small concentrations such as chondroitin sulfate, keratin sulfate and lipids (e.g., phospholipids, triglycerides, fatty acids, cholesterol, etc.) [27]. It needs to be noted that the samples that underwent EDX analysis did not consist of only pure hydroxyapatite; additionally, surface composition analysis can sometimes be misleading because of surface contamination [23].

5 CONCLUSIONS

The results presented in this article demonstrate the effect of the solubilization process on the structure of materials used in the experiments. The FTIR spectrum as well as SEM-EDX analysis confirm the influence of dose on the solubilization factor as well as the influence of the material used on the effectiveness of solubilization performed by *Bacillus megaterium*.

ACKNOWLEDGMENTS

This project is financed within the framework of grant PBS 2/A1/11/2013 entitled "Phosphorus renewable raw materials – a resource base for new generation of fertilizers," attributed by the National Center for Research and Development.

REFERENCES

1. H. Ge, D.J. Batstone, and J. Keller, Biological phosphorus removal from abattoir wastewater at very short sludge ages mediated by novel PAO clade Comamonadaceae. *Water Res.* **69**, 173–182 (2015).
2. A. Pettersson, L.-E. Åmand, and B.-M. Steenari, Leaching of ashes from co-combustion of sewage sludge and wood—Part I: Recovery of phosphorus. *Biomass Bioenerg.* **32**, 224–235 (2008).
3. J. Cooper, R. Lombardi, D. Boardman, and C. Carliell-Marquet, The future distribution and production of global phosphate rock reserves. *Resour. Conserv. Recy.* **57**, 78–86 (2011).
4. Z. Tan and A. Lagerkvist, Phosphorus recovery from the biomass ash: A review. *Renew Sust. Energ. Rev.* **15**, 3588–3602 (2011).
5. R.P. Viader, P.E. Jensen, L.M. Ottosen, J. Ahrenfeldt, and H. Hauggaard-Nielsen, Electrodialytic extraction of phosphorus from ash of low-temperature gasification of sewage sludge. *Electrochim. Acta* **181**, 100–108 (2015).
6. H. Herzel, O. Krüger, L. Hermann, and C. Adam, Sewage sludge ash—A promising secondary phosphorus source for fertilizer production. *Sci. Total Environ.* **542**, 1136–1143 (2016).
7. M. Wyciszkiewicz, A. Saeid, J. Dobrowolska-Iwanek, and K. Chojnacka, Utilization of microorganisms in the solubilization of low-quality phosphorus raw material. *Ecol. Eng.* **89**, 109–113 (2016).
8. B.C. Behera, S.K. Singdevsachan, R.R. Mishra, S.K. Dutta, and H.N. Thatoi, Diversity, mechanism and biotechnology of phosphate solubilising microorganism in mangrove—A review. *Biocatal. Agric. Biotechnol.* **3**, 97–110 (2014).
9. G.-C. Tao, Sh.-J. Tian, M.-Y. Cai, and G.-H. Xie, Phosphate-solubilizing and -mineralizing abilities of bacteria isolated from soils. *Pedosphere* **18**, 515–523 (2008).
10. M. Wyciszkiewicz, A. Saeid, K. Chojnacka, and H. Górecki, Production of phosphate biofertilizers from

bones by phosphate-solubilizing bacteria *Bacillus megaterium*. *Open Chem.* **13**, 1063–1070 (2015).
11. A. Saeid, M. Labuda, K. Chojnacka, and H. Górecki, Valorization of bones to liquid phosphorus fertilizer by microbial solubilization. *Waste Biomass Valor.* **5**, 265–272 (2014).
12. T. Yin, J.W. Park, and S. Xiong, Physicochemical properties of nano fish bone prepared by wet media milling. *LWT-Food Sci. Technol.* **64**, 367–373 (2015).
13. R. Abraham, J. George, J, Thomas, and K.K.M Yusuff, Physicochemical characterization and possible applications of the waste biomass ash from oleoresin industries of India. *Fuel* **109**, 366–372 (2013).
14. S. Patel, J. Han, W. Qiu, and W. Gao, Synthesis and characterisation of mesoporous bone char obtained by pyrolysis of animal bones, for environmental application. *J. Environ. Chem. Eng.* **3**, 2368–2377 (2015).
15. N.L. D'Elía, A.N. Gravina, J.M. Ruso, J.A. Laiuppa, G.E. Santillán, and P.V. Messina, Manipulating the bioactivity of hydroxyapatite nano-rods structured networks: Effects on mineral coating morphology and growth kinetic. *BBA-Gen. Subjects* **1830**, 5014–5026 (2013).
16. T.G.M. Bonadio, F. Sato, A.N. Medina, W.R. Weinand, M.L. Baesso, and W.M. Lima, Bioactivity and structural properties of nanostructured bulk composites containing Nb_2O_5 and natural hydroxyapatite. *J. Appl. Phys.* **113**, 223505 (2013).
17. M. Boutinguiza, J. Pou, R. Comesaña, F. Lusquiños, A. de Carlos, and B. León, Biological hydroxyapatite obtained from fish bones. *Mater. Sci. Eng.* **32**, 478–486 (2012).
18. H. Galai and F. Slima, Mineral characterization of the Oum El Khacheb phosphorites (Gafsa-Metlaoui basin; S Tunisia). *Arabian J. Chem.* **1** (2014). doi: 10.1016/j.arabjc.2014.10.007
19. H.K. Lim, T.T. Teng, M.H. Ibrahim, A. Ahmad, and H.T. Chee, Adsorption and removal of zinc (II) from aqueous solution using powdered fish bones. *APCBEE Procedia* **1**, 96–102 (2012).
20. T.-P. Chung, C.-Y. Wu, and R.-S. Juang, Improved dynamic analysis on cell growth with substrate inhibition using two-phase models. *Biochem. Eng. J.* **25**, 209–217 (2005).
21. D. Pienkowski, T.M. Doers, M.-C. Monier-Faugere, Z. Geng, P. Nancy, B.A.L. Camacho, and H.H. Malluche, Calcitonin alters bone quality in beagle dogs. *J. Bone Miner. Res.* **12**, 1936–1943 (1997).
22. P. Álvarez-Lloret, A.B. Rodríguez-Navarro, Ch.S. Romanek, K.F. Gaines, and J. Congdon, Quantative analysis of bone mineral using FT-IR. *MACLA* **6**, 45–47 (2006).
23. H. Zeng and W.R. Lacefield, XPS, EDX and FT-IR analysis of pulsed laser deposited calcium phosphate bioceramic coatings: The effects of various process parameters. *Biomaterials* **21**, 23–30 (2000).
24. N.A.M. Barakat, K.A. Khalil, F.A. Sheikh, A.M. Omran, G, Babita, S.M. Khil, and H.Y. Kim, Physiochemical characterizations of hydroxyapatite extracted from bovine bones by three different methods: Extraction of biologically desirable HAp. *Mater. Sci. Eng. C* **28**, 1381–1387 (2008).
25. B. Kizilkaya, A.A. Tekinay, and Y. Dilginc, Adsorption and removal of Cu (II) ions from aqueous solution using pretreated fish bones. *Desalination* **264**, 37–47 (2010).
26. M.B. Jabłoński, E.A. Stefaniak, L. Darchuk, K. Turżańska, M. Gorzelak, R. Kuduk, Dorriné, and R. Van Grieken, Microchemical investigation of bone derived from mice treated with strontium in different chemical forms using scanning electron microscopy and micro-Raman spectroscopy. *Microchem. J.* **108**, 168–173 (2013).
27. N.A.M. Barakat, M.S. Khil, A.M. Omran, F.A. Sheikhd, and H.Y. Kima, Extraction of pure natural hydroxyapatite from the bovine bones bio waste by three different methods. *J. Mater. Process. Technol.* **209**, 3408–3415 (2009).